

Nonlinearly broadened phase-modulated continuous-wave laser frequency combs characterized using DPSK decoding

Chen-Bin Huang¹, Sang-Gyu Park^{1,2}, Daniel E. Leaird¹, and Andrew M. Weiner¹

¹ School of Electrical and Computer Engineering, Purdue University
465 Northwestern Ave., West Lafayette, IN 47907-2035

² Division of Electronics and Computer Engineering, Hanyang University, Seoul, Korea
robinh@purdue.edu, leaird@purdue.edu, sanggyu@hanyang.ac.kr, amw@purdue.edu

Abstract: 9.953 GHz phase-modulated continuous-wave laser combs are spectrally broadened via nonlinear propagation in normal and anomalous dispersion media and experimentally characterized using a differential phase shift keying (DPSK) decoder. DPSK bit-error rate data are in qualitative agreement with radio-frequency spectrum analyzer measurements.

© 2008 Optical Society of America

OCIS codes: (060.2330) Fiber optical communications; (320.7110) Ultrafast nonlinear optics; (060.7140) Ultrafast processes in fibers; (060.5530) Pulse propagation and solitons

References and links

1. R. A. Linke and A. H. Gnauck, "High-capacity coherent lightwave systems," *J. Lightwave Technol.* **6**, 1750–1769 (1988).
2. H. Toba, K. Oda, and K. Nosu, "Design and performance of FSK-direct detection scheme for optical FDM systems," *J. Lightwave Technol.* **9**, 1335–1343 (1991).
3. T. Chikama, S. Watanabe, T. Naito, H. Onaka, T. Kiyonaga, Y. Onoda, H. Miyata, M. Suyama, M. Seino, and H. Kuwahara, "Modulation and demodulation techniques in optical heterodyne PSK transmission systems," *J. Lightwave Technol.* **8**, 309–325 (1990).
4. A. H. Gnauck and P. J. Winzer, "Optical phase-shift-keyed transmission," *J. Lightwave Technol.* **23**, 115–130 (2005).
5. M. Mlejnek, "Balanced differential phase-shift keying detector performance: an analytical study," *Opt. Lett.* **31**, 2266–2268 (2006).
6. S. Weisser, S. Ferber, L. Raddatz, R. Ludwig, A. Benz, C. Boerner, and H. G. Weber, "Single- and alternating polarization 170 Gb/s transmission up to 4000 km using dispersion-managed fiber and all-Raman amplification," *IEEE Photon. Technol. Lett.* **18**, 1320–1322 (2006).
7. H. G. Weber, S. Ferber, M. Kroh, C. Schmidt-Langhorst, R. Ludwig, V. Marembert, C. Boerner, F. Futami, S. Watanabe, and C. Schubert, "Single channel 1.28 T/s and 2.56 Tb/s DQPSK transmission," *Electron. Lett.* **42**, 178–179 (2006).
8. H. G. Weber, R. Ludwig, S. Ferber, C. Schmidt-Langhorst, M. Kroh, V. Marembert, C. Boerner, and C. Schubert, "Ultrahigh-speed OTDM-transmission technology," *J. Lightwave Technol.* **24**, 4616–4627 (2006).
9. F. Quinlan, S. Gee, S. Ozharar, and P. J. Delfyett, "Ultralow-jitter and -amplitude-noise semiconductor-based actively mode-locked laser," *Opt. Lett.* **31**, 2870–2872 (2006).
10. S. Gee, S. Ozharar, F. Quinlan, J. J. Plant, P. W. Juodawlkis, and P. J. Delfyett, "Self-stabilization of an actively mode-locked semiconductor-based fiber-ring laser for ultralow jitter," *IEEE Photon. Technol. Lett.* **19**, 498–500 (2007).
11. K.R. Tamura, H. Kubota and M. Nakazawa, "Fundamentals of stable continuum generation at high repetition rate," *IEEE J. Quantum Electron.* **36**, 773–779 (2000).
12. F. Futami and K. Kikuchi, "Low-noise multiwavelength transmitter using spectrum-sliced supercontinuum generated from a normal group-velocity dispersion fiber," *IEEE Photon. Technol. Lett.* **13**, 73–75 (2001).
13. H. Sotobayashi and K. Kitayama, "Observation of phase conservation in multiwavelength binary phase shift-keying pulse-sequence generation at 10 Gbits/s by use of a spectrum-sliced supercontinuum in an optical fiber," *Opt. Lett.* **24**, 1820–1822 (1999).
14. T. Kuri, T. Nakasyotani, H. Toda and K. Kitayama, "Characterization of supercontinuum light source for WDM millimeter-wave-band radio-over-fiber systems," *IEEE Photon. Technol. Lett.* **17**, 1274–1276 (2005).
15. K. L. Corwin, N. R. Newbury, J. M. Dudley, S. Coen, S. A. Diddams, K. Weber, and R. S. Windeler, "Fundamental noise limitations to supercontinuum generation in microstructure fiber," *Phys. Rev. Lett.* **90**, 113904 (2003).
16. N. R. Newbury, B. R. Washburn, K. L. Corwin, and R. S. Windeler, "Noise amplification during supercontinuum generation in microstructure fiber," *Opt. Lett.* **28**, 944–946 (2003).

17. D. M. Baney and W. V. Sorin, "High resolution optical frequency analysis," in *Fiber Optic Test and Measurement*, D. Derickson, ed., (Prentice Hall, 1998), pp.169-219.
18. H. Murata, A. Morimoto, T. Kobayashi, and S. Yamamoto, "Optical pulse generation by electrooptic-modulation method and its application to integrated ultrashort pulse generators," *IEEE J. Sel. Top. Quantum Electron.* **6**, 1325-1331 (2000).
19. T. Sakamoto, T. Kawanishi, and M. Izutsu, "Asymptotic formalism for ultraflat optical frequency comb generation using a Mach-Zehnder modulator," *Opt. Lett.* **32**, 1515-1517 (2007).
20. C.-B. Huang, Z. Jiang, D. E. Leaird, and A. M. Weiner, "High-rate femtosecond pulse generation via line-by-line processing of a phase-modulated CW laser frequency comb," *Electron. Lett.* **42**, 1114-1115 (2006).
21. J. van Howe, J. H. Lee, and C. Xu, "Generation of 3.5 nJ femtosecond pulses from a continuous-wave laser without mode-locking," *Opt. Lett.* **32**, 1408-1410 (2007).
22. Z. Jiang, C.-B. Huang, D. E. Leaird, and A. M. Weiner, "Optical arbitrary waveform processing of more than 100 spectral comb lines," *Nature Photon.* **1**, 463-467 (2007).
23. D. Miyamoto, K. Mandai, T. Kurokawa, S. Takeda, T. Shioda, and H. Tsuda, "Waveform-controllable optical pulse generator using an optical pulse synthesizer," *IEEE Photon. Technol. Lett.* **18**, 721-723 (2006).
24. N. K. Fontaine, R. P. Scott, J. Cao, A. Karalar, W. Jiang, K. Okamoto, J. P. Heritage, B. H. Kolner, and S. J. B. Yoo, "32 phase X 32 amplitude optical arbitrary waveform generation," *Opt. Lett.* **32**, 865-867 (2007).
25. S. V. Chernikov and P. V. Mamyshev, "Femtosecond soliton propagation in fibers with slowly decreasing dispersion," *J. Opt. Soc. Am. B* **8**, 1633-1641 (1991).
26. J. J. O. Pires and J. R. F. da Rocha, "Performance analysis of DPSK direct detection optical systems in the presence of interferometric intensity noise," *J. Lightwave Technol.* **10**, 1722-1730 (1992).
27. D. von der Linde, "Characterization of the noise in continuously operating mode-locked lasers," *Appl. Phys. B* **39**, 201-217 (1986).
28. K. R. Tamura and M. Nakazawa, "Femtosecond soliton generation over a 32-nm wavelength range using a dispersion-flattened dispersion-decreasing fiber," *IEEE Photon. Technol. Lett.* **11**, 319-321 (1999).

1. Introduction

Coherent communications have been extensively studied in the 1980s and early 1990s in optical fiber communication systems [1,2]. Among various data encoding formats, differential-phase-shifted-keying (DPSK) is an optical phase-only data modulation format in which the optical phase changes between adjacent bits are used for data decoding [3,4]. Using balanced detection, DPSK has the advantage of a 3-dB lower optical signal-to-noise-ratio requirement as compared to the conventional ON-OFF-keying approach [4,5]. The 3-dB sensitivity advantage enables DPSK systems with longer fiber reach and with lower transmitted power, being less susceptible to fiber nonlinearities.

Recently, interest in coherent ultrashort pulse communications (especially employing phase shift keying) has reemerged as a means for achieving extremely high bit-rate systems (ranging from a few hundreds of Gb/s to over 1Tb/s) over long fiber transfer links [6-8]. In such high rate demonstrations, the approach is to start with pulse generators at a base repetition rate (10~40Gbit/s) followed by subsequent optical time-domain multiplexing (OTDM) to obtain the multiplied transmission rate. As a result, it is crucial that the pulse sources provide stable repetition rate and wavelength, pulse-width significantly shorter than the multiplexed bit period, high pulse energy extinction ratio, and timing jitter much less than the pulse width. Careful characterizations of the pulse sources are thus required.

Conventionally, 10~40 GHz optical pulse trains have been derived from mode-locked lasers (therefore generating optical frequency combs, with comb lines spaced apart by the pulse repetition frequency). However, significant effort is needed to stabilize lasers with multi-GHz-mode-locked repetition rates typically achieved via harmonic mode-locking [9,10]. To obtain shorter pulses for Tb/s OTDM systems, ps-duration pulses directly obtained through mode-locked frequency combs are subsequently sent through nonlinear fiber propagation for spectral broadening. Such nonlinearly broadened combs have been widely explored [11-16]. Typically, comb properties have been characterized using spectral slicing followed by measurements on an electrical spectrum analyzer (ESA) [11,14-16], on-off keying [12], or a scanning Fabry-Perot filter [11]. Such characterization techniques are sensitive predominantly to intensity noise and timing jitter. Phase conservation in the comb broadening process has been examined through binary phase encoding the time-multiplexed seed pulses which are decoded and characterized subsequent to nonlinear propagation [13]. Laser linewidth

measurements using direct heterodyne beating or delayed self-{homodyne, heterodyne} are also well developed techniques [17].

More recently, much interest have been focused on optical frequency comb generation using externally-modulated continuous-wave lasers [18,19]. In contrast to harmonically mode-locked lasers, no frequency stabilization mechanisms are required for the externally-modulated scheme. This results in substantial flexibility for tuning line spacing, center wavelength, and optical bandwidth, which is useful for many applications [20-24].

In this paper, we discuss 10-GHz pulse sources, potentially useful for short pulse coherent communications, generated using 2.5ps transform-limited phase-modulated continuous-wave (PMCW) seed pulses followed by subsequent nonlinear spectral broadening using either normal or anomalous dispersion fibers. The pulses spectrally broadened in normal dispersion fiber shows substantially better DPSK performance compared to the anomalous dispersion fiber. These differences are related to data obtained using other comb characterization methods, primarily those based on radio frequency spectrum analysis. Our results show that DPSK encoding/decoding is a useful addition to the suite of comb characterization tools, since comb coherence, intensity noise, and timing jitter are all accounted for in the DPSK decoding process.

2. Experimental setup

Figure 1 shows a schematic diagram of our experimental setup. PMCW seed pulses are sent to a nonlinear medium for spectral broadening. Two nonlinear media are considered within this paper: (1) A commercially available dispersion decreasing fiber (DDF) of 2 km used for adiabatic soliton compression [25], with linearly decreasing dispersion values of 10 to 1.5 ps/nm/km from the input to the output. (2) A normal group velocity dispersion highly nonlinear fiber (HNLF) of 247 m, in which self-phase modulation is exploited as the broadening mechanism. The nonlinear coefficient of the HNLF is 10.5 (W km)^{-1} , the dispersion and the dispersion slope are -1.88 ps/nm/km and $0.016 \text{ ps/nm}^2/\text{km}$ respectively. After the nonlinear media, a grating based shaper is used to perform spectral slicing of the broadened combs. The spectrally sliced pulses are temporally phase-encoded with $\{0 \text{ or } \pi\}$ using a pseudo-random bit stream of length $2^{23}-1$ by a lithium niobate phase-modulator. The DPSK decoder is a commercial Michelson interferometer implemented in micro-optics, with delay τ_0 tuned exactly equal to one period of the PMCW pulse train. The DPSK decoder is operated single-ended; a single output is sent to a photo-detector (7.5 GHz bandwidth), followed by a limiting amplifier and measured using a bit-error-rate (BER) test set.

The setup for generating the 2.52 ps transform-limited PMCW seed pulse train at repetition rate $f_{\text{rep}}=9.953 \text{ GHz}$ is illustrated in Fig. 1(b). A CW laser (Koheras Adjustik: 1542 nm) with 1 kHz linewidth is sent to a dual-modulation comb generator, where a low- V_π phase modulator is driven at $2f_{\text{rep}}$ to obtain a wider comb bandwidth, and a subsequent intensity modulator is driven at f_{rep} to fill in the f_{rep} comb lines. A Fourier-Transform based spectral line-by-line pulse shaper is used to correct the phases of each spectral line of the PMCW comb using an automated process [20,22]. The resulting comb spectrum and the intensity autocorrelation of the pulse are shown in Figs. 1(c), 1(d), respectively. In Fig. 1(d), the calculated trace is obtained from Fig. 1(c) assuming a flat spectral phase, from which a deconvolved pulse duration of 2.52 ps is derived. The experimental trace coincides with the calculated trace, demonstrating high fidelity line-by-line phase shaping capability. A low noise erbium-doped fiber amplifier (EDFA1) is used to amplify the signal after the pulse shaper to 12 dBm (input -18 dBm), and subsequently a high gain EDFA (EDFA2, Pritel FP-400) with 20.5 dBm maximum output power is used after the line-by-line shaper followed by an optical filter with 4 nm bandwidth for elimination of optical amplifier noise. We estimate the optical signal to noise ratio (OSNR) of the PMCW comb after amplification to be approximately 30 dB, measured by using an OSA with resolution of 0.01 nm.

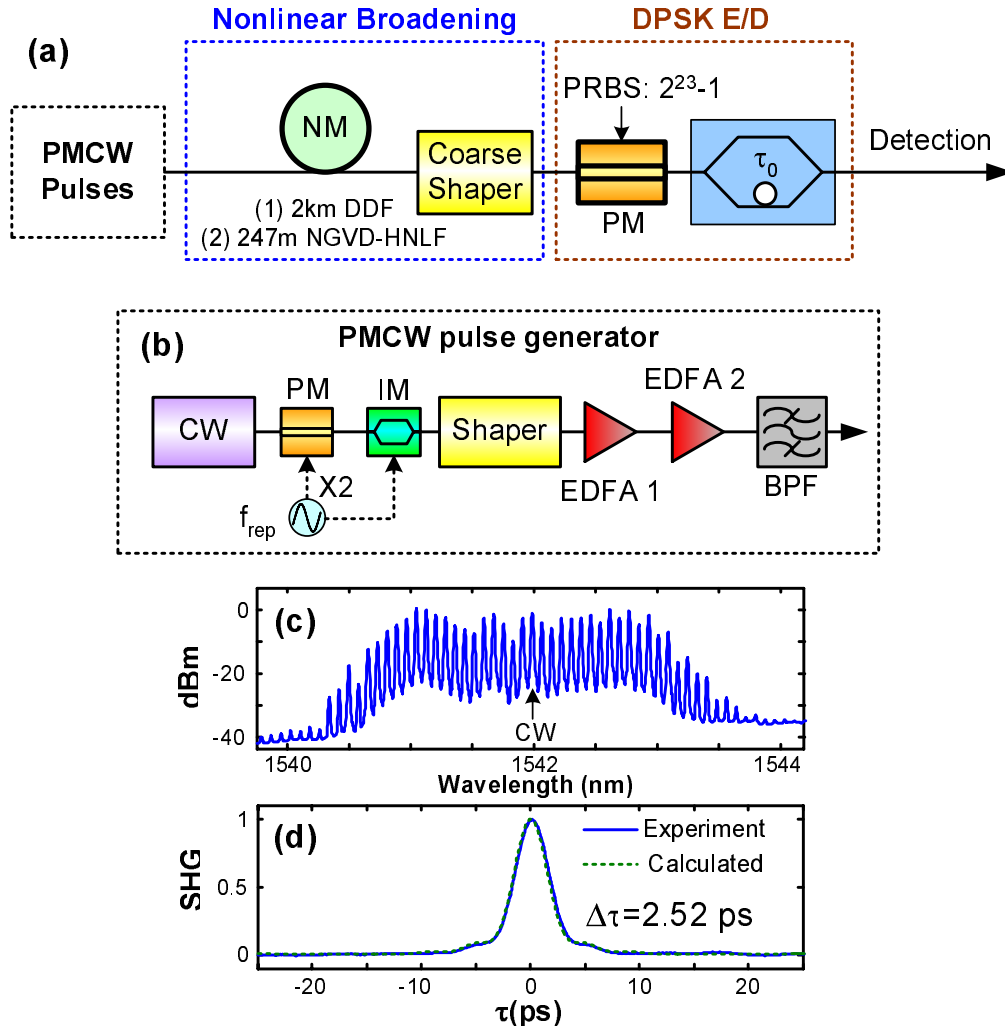


Fig. 1. Schematic of experimental setup. NM: nonlinear media; E/D: encoder/decoder. (b) PMCW pulse generation using a line-by-line shaper. PM: phase modulator; IM: intensity modulator; f_{rep} : comb spacing. (c) PMCW comb power spectrum. (d) Experimental (solid) and calculated (dash) intensity autocorrelation of the PMCW pulses.

3. Results and discussions

Figure 2(a) shows the nonlinearly broadened comb spectra after the DDF and HNLF with average seed pulse power of 18 dBm for both cases. This input power is sufficient to place our PMCW seed pulses into adiabatic soliton compression regime. Both combs provide ~ 8 nm optical bandwidth within -10 dB off the peak with the optical spectrum analyzer set for 0.01nm (1.25GHz) resolution. The PMCW comb is also included for comparison. DDF and HNLF comb portions at 1538 nm are magnified within the inset. Experimental (solid) and calculated (dashed) intensity autocorrelations of the corresponding pulses are shown in Fig. 2(b). The calculated curves are obtained using the measured optical power spectrum, with the assumption of flat spectral phase. For the HNLF-broadened comb, a coarse resolution pulse shaper is used to compensate the quadratic and slight cubic spectral phase as a result of self-phase modulation. De-convolved pulse widths of 415 and 526 fs are obtained for DDF and

HNLF, respectively. Such short pulse widths are desirable for ultrafast time-division multiplexed communications.

To assess compatibility with short pulse coherent communications, phase-coding and DPSK decoding are performed on both comb outputs. Figures 3(a) and 3(b) show DPSK decoded BER data (symbols) and fitting curves (lines) for the DDF comb, for various optical power levels (up to -12.0 dBm) at the receiver, and for the HNLF comb, respectively. BER results for the PMCW comb are also plotted in both figures for comparison. Considering Fig. 3(a), the DPSK performance suffers a power penalty of ~ 5 dB as compared to the PMCW comb when the entire DDF comb is used (All, diamond). Intuitively, different spectral portions may exhibit different comb qualities, and increased degradation is expected further into the wings. Spectral slicing (2 nm per different spectral regions of interest) is now performed to examine the spectral dependence of the comb quality. BER results show that the portion of the broadened spectrum coincident with the original PMCW comb (DDF 1542 nm) has better performance than using the whole comb, but still suffers a ~3 dB power penalty as compared to PMCW comb. DDF spectral slices centered at 1546 and 1538 nm have an evident larger power penalty.

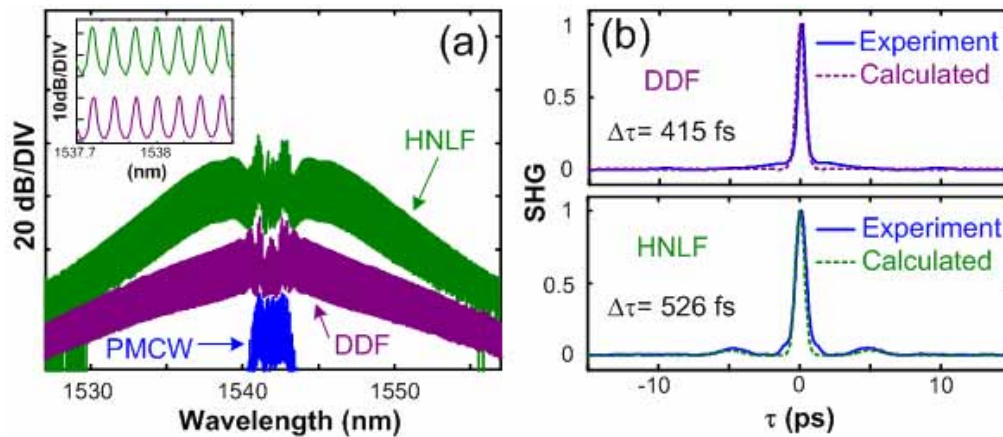


Fig. 2. (a). Nonlinearly broadened comb spectra. Inset: magnified 1538 nm DDF and HNLF comb portions. (b). Intensity autocorrelations of the DDF and HNLF pulses.

Figure 3(b) shows DPSK BER results for the HNLF comb. Excellent DPSK performance is obtained using either the entire HNLF comb (All, solid diamond) or any of the spectral slices, with less than 0.7 dB power penalties as compared to the PMCW comb results. We attribute this pronounced difference to the fact that modulational instability does not exist in the normal group velocity dispersion HNLF, in contrast to the comb broadened in the anomalous dispersion DDF.

Various mechanisms may contribute to the differences in DPSK performance between the two nonlinearly broadened combs which have comparable optical bandwidth. In order to gain further insight, conventional comb diagnostic methods used within Refs. [11,14-16] are also performed. First, the optical linewidths of different comb portions are measured via heterodyne beating with a reference CW laser with 15 MHz linewidth. For all the DDF and HNLF comb spectral portions, linewidths are determined to be narrower than this 15 MHz instrumental limit. Ref. [26] reports that 75 MHz laser linewidth results in ~1 dB power penalty at BER=10⁻⁹ for a 10 GHz DPSK system. Since the upper bound for our linewidths are well below this 75 MHz figure, we attribute the degradation of the DDF comb under DPSK operation to other mechanisms.

Secondly, relative intensity noise of the comb spectral slices is measured using an electrical spectrum analyzer. Figure 3(c) shows intensity noise power spectral densities for PMCW, DDF comb spectral slices, and the system noise floor, plotted against offset

frequency ranging from $\{-5 \text{ to } 5\}$ MHz relative to 9.953 GHz (resolution bandwidth=3 kHz). For all comb portions considered, optical powers of -3 dBm are fed to a 60 GHz bandwidth photo-detector. For the PMCW comb, only slight low-frequency noise is observed. All spectrally sliced portions of the DDF comb show both increased low-frequency noise and a white noise floor. Such noise measurement data have been previously interpreted in terms of slow variation in overall pulse energy (due to low frequency technical noise) and fast pulse structure variations (from white high frequency noise) [15,16]. Figure 3(d) shows intensity noise power spectral densities for HNFLF comb spectral slices. HNFLF comb low frequency noise pedestals are magnified in the inset of Fig. 3(d), along with the PMCW result (dashed trace) to facilitate comparison. No white noise backgrounds are observed, and only slight low-frequency noise pedestals are observed for 1538 and 1546 nm spectral slices. These observations qualitatively agree with the comb optical spectral measurements, where degradation in OSNR is observed for the DDF comb as compared to the HNFLF comb. Taking the 1538 nm spectral slice for example [inset, Fig. 2(a)], the optical extinction ratio is about 20 dB for the DDF comb but 23 dB for the HNFLF comb, as measured using OSA setting in 1.25GHz resolution. Increased RF noise from ESA measurements may be in part due to the beating of optical comb lines with the optical noise between the lines. From the inset of Fig. 3(d), the 1546 nm and 1538 nm slices have increased low frequency noise (roughly 6 dB) as compared to the 1542 nm and PMCW comb. This is consistent with the slight power penalties for the 1546 nm and 1538 nm spectral slides (by roughly 0.3 dB), which are apparent in the expanded BER curves plotted in Fig. 3(e).

Our third concern is timing jitter. Unlike NRZ-like coherent communications with long pulses, precise time alignment in the DPSK decoder is of critical importance for short pulse communication systems. Hence short pulse coherent communications is expected to be highly sensitive to timing jitter. Root-mean-square timing jitter values are shown in Table 1 for different portions of the comb. These timing jitter values are obtained by integrating the single-sided noise power spectral density within the frequency range $\{100 \text{ Hz} \sim 1 \text{ MHz}\}$ for each of the first four RF harmonics. As is well known [27], the timing jitter may be identified as the contribution to the integrated noise density that grows quadratically with harmonic number. The measured timing jitter values are qualitatively consistent with the DPSK BER results: both the full DDF comb and the various spectral slices of the comb have significantly increased jitter compared to the initial PMCW comb (63.13 fs) as well as significantly degraded BER performance. The increased intensity noise [Fig. 3(c)] may also contribute to the observed power penalties. Note however that both the timing jitter and BER data are noticeably worse for 1538 nm and 1546 nm spectral slices of the DDF comb compared to the 1542 nm spectral slide. However, the increase in intensity noise appears to be comparable for all three slices. This suggests that increased timing jitter for the DDF comb is a key factor impacting BER performance. In contrast, the various HNFLF spllices all retain low timing jitter similar to the initial PMCW comb, which is consistent with their excellent BER performance under DPSK decoding.

It is interesting to note that our DDF results are in apparent contrast to those reported by Refs. [7] and [11], where DDF have been successfully used to generate pulses for transmission experiments at greater than 1 Tb/s and where DDF-generated supercontinuum was reported to exhibit favorable noise properties, respectively. Although the reasons for this discrepancy are not known, we would like to point out three reasons that may contribute to the resolution of these differences:

(1) Dispersion tailoring of the DDFs may play a critical role in the spectrally broadened comb properties. In Ref. [11], specially engineered anomalous dispersive DDF with varying core shapes were fabricated during drawing; while in Ref. [28], dispersion-flattened DDFs with W-shaped core were used to generate a broad output spectrum. Such special DDFs are not generally available. The conclusion of Ref. [11] was the DDF resulted in supercontinuum with much lower noise compared to a normal dispersion fiber with dispersion value of almost zero. However, it has also been demonstrated by working in a larger normal dispersion value regime (similar to the case for our HNFLF) that supercontinuum can be generated both with

well preserved phase coherence and with low amplified incoherent noise and low intensity fluctuations [12,13].

(2) The requirements on the OSNR of the seed comb may be more demanding for DDF than for HNLF. In Ref. [11], it was shown that a 30 dB OSNR at the input to the DDF generated a high quality output comb from the DDF, but when the OSNR was intentionally lowered to 23 dB the output comb was seriously degraded. The OSNR of our seed PMCW comb (~30 dB) is comparable to the condition described in Ref. [11]. Therefore, OSNR would not appear to explain the difference between our results and that of [11], unless OSNR requirements vary significantly with details of the DDF dispersion profile.

(3) For adiabatic soliton compression, the shape of the input seed pulse may also be an important factor. Ideally, adiabatic soliton compression works for pulses showing sech temporal field profile. In the prior studies using DDF, seed pulses have been generally obtained from mode-locked laser outputs, where the pulses generally show high extinction ratio and are either sech or Gaussian in shape. PMCW seed pulses, however, owing to the comb spectral profile, are expected to have a different shape with larger pulse pedestals. This deviation from the soliton profile may also contribute to the degraded coherence and increased background noise observed in our DDF compressed comb. On the other hand, normally dispersive HNLF does not have an inherent requirement on the input seed pulse shape. In any case, clarification of the conditions needed to preserve low noise in compression using DDF remains an important open research question.

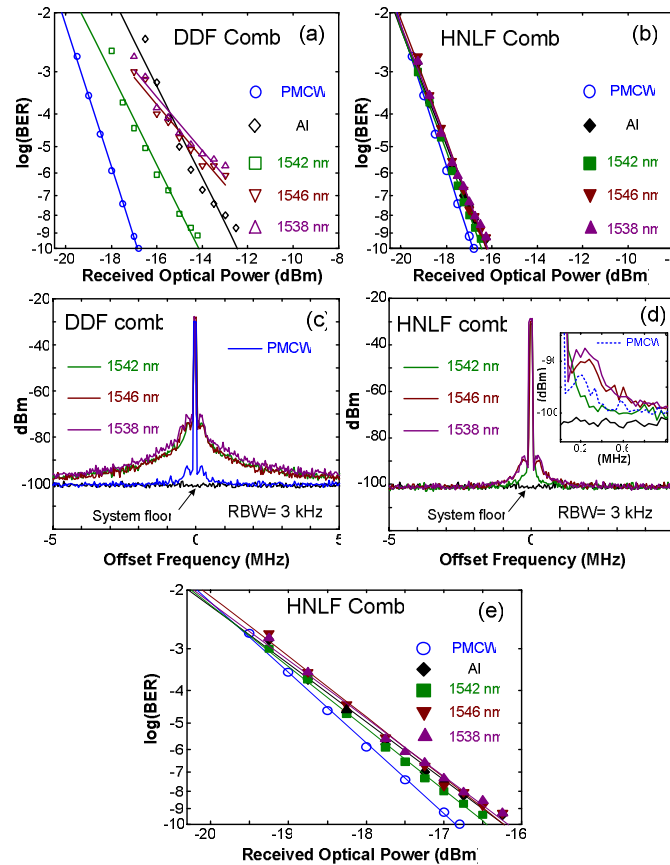


Fig. 3. DPSK decoded BER results of (a) PMCW and DDF combs; (b) HNLF comb. In (a, b), data are denoted by symbols and lines the fitted BER curve. Intensity noise measurements of different comb portions for: (c) PMCW and DDF comb and (d) HNLF comb PMCW (inset). (e) Magnified view of the HNLF comb BER results.

Table 1. Corresponding rms timing jitter values for different comb portions integrated from 100 Hz to 1 MHz for different comb portions.

Comb Portion	Time jitter (fs)
PMCW	63.13
DDF All	116.00
DDF 1542 nm	109.99
DDF 1546 nm	165.34
DDF 1538 nm	175.42
HNLF All	78.87
HNLF 1542 nm	65.60
HNLF 1546 nm	65.43
HNLF 1538 nm	82.93

4. Conclusion

In summary, we have characterized two different frequency combs, generated via phase modulation of a continuous-wave laser and spectrally broadened in either dispersion-decreasing fiber or normal dispersion highly nonlinear fiber, via a variety of methods. Our results show that the BER performance of the dispersion-decreasing fiber version in a simple DPSK system is severely compromised, while the BER characteristics of the comb broadened using normal dispersion fiber are essentially unaffected. An important point is that these experiments with DDF and with HNLF were performed with identical input. These observations are consistent with measurements of intensity noise and timing jitter based on radio-frequency spectral analysis. Although it may be possible to obtain better results with DDF under different conditions, as reported in the literature, our results point to PMCW combs spectrally broadened using normal dispersion fiber (and subsequently compressed) as a promising and robust source for ultrashort pulse coherent communications. At the same time, our work shows that DPSK decoding, which accounts for intensity noise, timing jitter, and linewidth degradations within one single process, may be a valuable addition to the suite of tools available for characterization of optical comb sources.

Acknowledgment

This work was supported by the National Science Foundation under Grant ECCS-0601692. A. M. Weiner acknowledges helpful discussions with Scott A. Diddams and Leo Hollberg at NIST-Boulder, Colorado.